Gene 573 (2015) 115–122

Contents lists available at ScienceDirect

Gene

journal homepage: www.elsevier.com/locate/gene

Research paper

Transactivation activity and nucleocytoplasmic transport of β-catenin are independently regulated by its C-terminal end

J.L. Maturana [a], I. Niechi [a], E. Silva [a], H. Huerta [a], R. Cataldo [a], S. Härtel [b], L.F. Barros [c], M. Galindo [a], J.C. Tapia [a,*]

[a] Program of Cellular and Molecular Biology, ICBM, Faculty of Medicine, University of Chile, Santiago, Chile
[b] Laboratory for Scientific Image Analysis (SCIAN-Lab), ICBM, Faculty of Medicine, University of Chile, Santiago, Chile
[c] Centro de Estudios Cientificos, Valdivia, Chile

ARTICLE INFO

Article history:
Received 12 June 2015
Accepted 11 July 2015
Available online 15 July 2015

Keywords:
β-Catenin
Nucleocytoplasmic
Phosphorylation
CK2

ABSTRACT

The key protein in the canonical Wnt pathway is β-catenin, which is phosphorylated both in absence and presence of Wnt signals by different kinases. Upon activation in the cytoplasm, β-catenin can enter into the nucleus to transactivate target gene expression, many of which are cancer-related genes. The mechanism governing β-catenin's nucleocytoplasmic transport has been recently unvealed, although phosphorylation at its C-terminal end and its functional consequences are not completely understood. Serine 646 of β-catenin is a putative CK2 phosphorylation site and lies in a region which has been proposed to be important for its nucleocytoplasmic transport and transactivation activity. This residue was mutated to aspartic acid mimicking CK2-phosphorylation and its effects on β-catenin activity as well as localization were explored. β-Catenin S6464D did not show significant differences in both transcriptional activity and nuclear localization compared to the wild-type form, but displayed a characteristic granular nuclear pattern. Three-dimensional models of nuclei were constructed which showed differences in number and volume of granules, being those from β-catenin S646D more and smaller than the wild-type form. FRAP microscopy was used to compare nuclear export of both proteins which showed a slightly higher but not significant retention of β-catenin S646D. Altogether, these results show that C-terminal phosphorylation of β-catenin seems to be related with its nucleocytoplasmic transport but not transactivation activity.

1. Introduction

The canonical Wnt pathway is involved in cell proliferation, cell fate decisions and differentiation (Logan and Nusse, 2004). The main effector in this pathway is β-catenin, which in the absence of Wnt signals is phosphorylated in its amino terminus by CK1α and GSK3β, events coordinated by the scaffold proteins Axin and APC. Phospho-β-catenin is ubiquitinated by TrCP-E3 ligase and thereby targeted to proteasomal degradation (Macdonald et al., 2009). Upon binding of Wnt ligands or misregulation of the degradation process, stabilized β-catenin import to the nucleus and activates transcription of many genes, which is a feature shared by different cancers, including colorectal (Bienz and Clevers, 2000), ovarian (Jamieson et al., 2004) and brain (Zhang et al., 2011).

Despite β-catenin does not contain any nuclear localization (NLS) or nuclear export sequence (NES), it can transport between cytoplasm and nucleus. β-Catenin has been suggested to be actively exported by these proteins through the CRM1/exportin-1 nuclear export pathway (Cong and Varmus, 2004; Henderson, 2000; Neufeld et al., 2000; Rosin-Arbesfeld et al., 2003; Thyssen et al., 2006; Wang et al., 2014). However, β-catenin can also export from nucleus in a CRM1-independent manner when no β-catenin binding partners are overexpressed as well as this movement is RanGTP-independent, which suggest that β-catenin could be also mediating its own transport through the nuclear pore complex (Eleftheriou et al., 2001; Wiechens and Fagotto, 2001).

Given that TCF-1, XTcf-3 and BCL9/Pygo can bind and retain β-catenin at the nucleus, it has been suggested that these proteins can indeed import it (Townsley et al., 2004), however, active transport has not been directly tested for them, by which nuclear import by retention was suggested to be the mechanism (Henderson and Fagotto, 2002). Regarding this, β-catenin was shown to bind BCL9 and TCF4 in the nucleus and thereby was enriched by retention (Krieghoff et al., 2006).

β-Catenin structure is formed by unstructured N- and C-terminal ends plus a central region composed of 12 copies (R1–R12) of a motif known as Armadillo (ARM) (Xing et al., 2008). On the other hand, β-

Abbreviations: CK2, protein kinase CK2 (formerly Casein Kinase 2); FRAP, fluorescence recovery after photobleaching; APC, adenomatous poliposis coli protein; ARM, Armadillo repeat; GFP, green fluorescent protein.

* Corresponding author at: Cell Transformation Laboratory, Program of Cellular and Molecular Biology, ICBM, Faculty of Medicine, University of Chile, Av. Independencia 1027, Santiago 8380453, Chile.
E-mail address: jtapia@med.uchile.cl (J.C. Tapia).

http://dx.doi.org/10.1016/j.gene.2015.07.039
0378-1119/

importin translocates into the nucleus by interaction with nucleoporins. β-importin is formed by HEAT repeats, whose repeats 4 to 8 are necessary and sufficient for its nuclear import (Cook et al., 2007). Interestingly, these HEAT repeats 4–8 contain a conformational resemblance with ARM repeats R8 to R12 from β-catenin (Lee et al., 2000). Moreover, a region conformed by R10–R12 plus the C-terminal end has been reported to have a key role in the nuclear/cytoplasmic shuttling of β-catenin, showing export and import rates similar to the full length protein (Koike et al., 2004).

CK2 enzyme is a Ser/Thr-kinase that phosphorylates over 300 proteins participating in many processes, such as replication, transcription, translation and signal transduction (Ahmed et al., 2002; Litchfield, 2003; Meggio and Pinna, 2003). CK2 participates as an important component of the canonical Wnt pathway by interacting and phosphorylating β-catenin at residue Thr393 (Gao and Wang, 2006; Seldin et al., 2005; Song et al., 2003), thereby promoting expression of key proteins involved in tumor progression, such as survivin, cyclin D and COX-2 (Tapia et al., 2006; Ponce et al., 2011; Yefi et al., 2011), between many others. Furthermore, phosphorylation by CK2 has been implicated in regulation of bi-directional movement between nucleus and cytoplasm for diverse proteins. For instance, CK2 has been reported to regulate nuclear import of APC, HMGB1, ERK1/2, Nrf2 (Apopa et al., 2008; De Abreu da Silva et al., 2011; Plotnikov and Chuderland, 2011; Zhang et al., 2001a) as well as nuclear export of NFATc, alphaNAC and S6K1 II (Panasyuk et al., 2006; Porter et al., 2000; Quélo et al., 2005).

Serine 646 in human β-catenin is a putative site of phosphorylation by CK2 (i.e., S/TXXD/E/^{P}S/^{P}T/^{P}Y; X = any, P = phosphorylated) which is located into the R12-ARM motif of this protein. Ser646 interacts through hydrogen bonds with Arg684 at the end of the helix C, which it has been suggested to be linked to the transactivation of β-catenin target genes (Xing et al., 2008). In this work, we evaluated whether Ser646 when phosphorylated may have a role in subcellular localization, nucleocytoplasmic transport and transcriptional activity. Our findings show that despite phospho-like β-catenin displays significantly more and smaller granules which seem to be also more retained at nuclei, this is unrelated with an increment of its transcriptional activity. Therefore, phosphorylation in different motifs of β-catenin may be related with its nucleocytoplasmic transport but not necessarily with its transactivation activity on cancer-related genes.

2. Results

2.1. Serine 646 of β-catenin is a putative phosphorylation site

An in silico analysis of β-catenin sequence showed the presence of a putative CK2 phosphorylation site, Ser646, located at the C-terminal end of ARM 12 (Fig. 1A). This residue matches well with the consensus sequence of phosphorylation for the protein kinase CK2 (Meggio and Pinna, 2003). Interestingly, an alignment of several β-catenin protein sequences showed that this Ser646 residue is highly conserved in different species (Fig. 1B). This suggested that phosphorylation by CK2 at Ser646 may be occurring at the C-terminal end of β-catenin, which also may have potential outcomes in both normal and pathological conditions. Therefore, β-catenin was engineered to express aspartic acid (i.e., S646D) in this position in order to mimic phosphorylation.

2.2. Similar transactivating activity of β-catenin wild-type and S646D

To assess potential differences between β-catenin WT and S646D as co-activators of gene transcription, we measured mRNA and protein levels of survivin, which is a known β-catenin target (Tapia et al., 2006; Zhang et al., 2001b). HEK-293T cells over-expressing either β-catenin WT or S646D showed similar levels of mRNA and protein survivin (Fig. 2A,B) and only when compared to the mock expression they displayed differences in mRNA levels. Similar results were observed for mRNA and protein levels of other β-catenin targets, including

Fig. 1. Serine 646 in β-catenin is a putative site of CK2 phosphorylation. (A) Cartoon of β-catenin structure was constructed with PyMOL 1.5.0.4 software by using the PDB 2Z6H (Xing et al., 2008). β-Catenin structure starts from residue 149, with 12 ARM repeats conforming the Armadillo domain (blue) together the last portion of helix C (orange). Ser646 is indicated at the C-terminal region on R12-ARM repeat (red). (B) Sequence alignment of part of the R12-ARM repeat from several species, where the conserved Ser646 in human β-catenin is highlighted. Phosphorylation consensus sequence for CK2 is depicted with an asterisk (S/TXXE/D from Meggio and Pinna, 2003). Alignment was made using the CLUSTALX 2.1 software.

COX-2, ET-1 and cyclin D1 (data not shown). Also, survivin mRNA and protein levels correlated with results obtained with a luciferase reporter assay specific for survivin's promoter, where cells over-expressing β-catenin WT or S646D showed high levels of reporter activity compared to the mock transfected cells, with no significant differences between them (Fig. 2C).

2.3. Nuclear clustering of β-catenin S646D displays smaller granules

Subcellular localization of β-catenin WT and S646D was evaluated through confocal microscopy. Cells overexpressing each protein fused to GFP showed nuclear clustering with visible formation of rounded aggregates or "granules", displaying a particular pattern at difference of GFP-only expressing cells (Fig. 3). This pattern was irrespective of either different DNA concentrations or post-transfection incubation times (data not shown).

Given the particular β-catenin granule patterns observed, we characterized them by building three-dimensional (3D) models of the cell nuclei (Liddle et al., 2014). Thus, Z-stacks of the cells over-expressing β-catenin WT or S646D were acquired and then 3D-models (see Fig. 5C for reference) were constructed using software developed in the Interactive Data Language (IDL). After 3D reconstruction of the nuclei, the number, surface and volume of granules were determined. Compared to β-catenin WT, cells overexpressing β-catenin S646D showed a higher number of granules (Fig. 4A) as well as total granule surface per nucleus (Fig. 4B). Total volume occupied by these granules was similar in nuclei from both β-catenin WT and S646D (Fig. 4C), however, as expected the mean value of the single granule volume was different among the β-catenin variants (Fig. 4D). Thus, cells overexpressing β-catenin S646D exhibited the smallest value (0.13 μm^3) while cells overexpressing β-catenin WT the largest (0.22 μm^3).

A more detailed analysis of the single granule volume of the β-catenin WT and S646D showed a different distribution among them. Thus, single granule volumes showed values ranged from 0.05 to 0.60 μm^3, where cells over-expressing β-catenin WT presented the widest distribution of volumes, as well as the largest granules, displaying 15% of these by over 0.4 μm^3 (Fig. 5A). On the contrary, cells

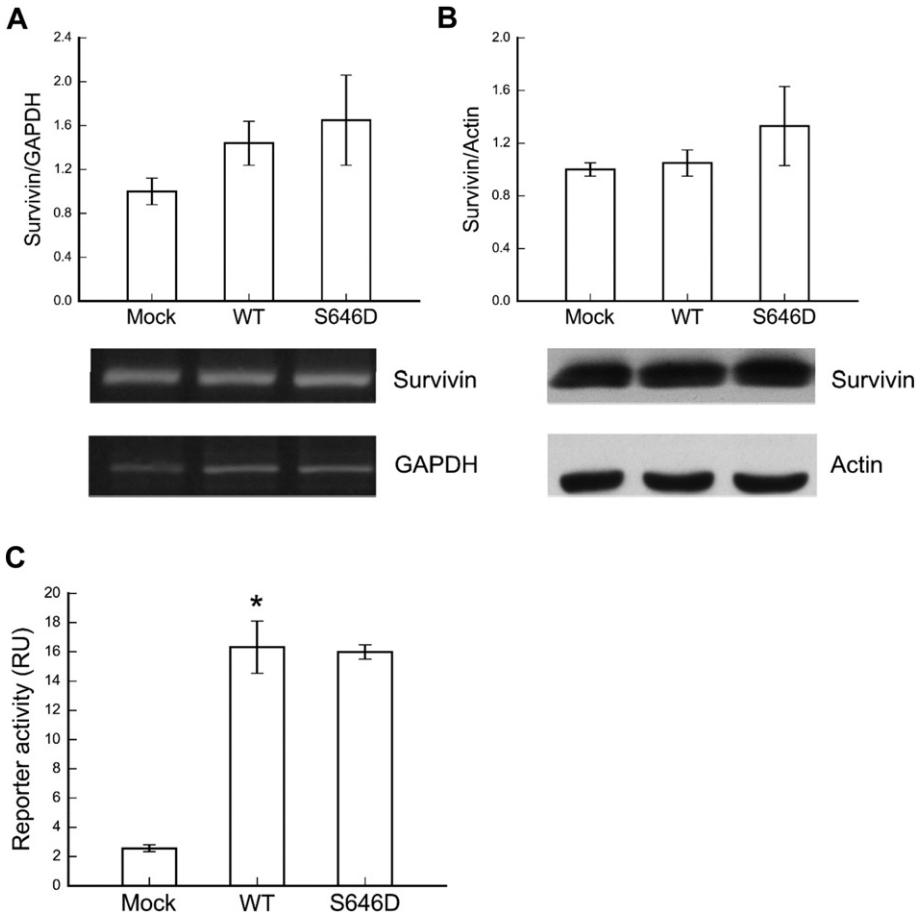

Fig. 2. Transactivating activity of β-catenin S646D. HEK-293T cells were transfected with 1 μg each plasmids encoding GFP-fused β-catenin wild-type or GFP-β-cat-S646D. Twenty-four hours post-transfection, mRNA (A) and proteins (B) were collected and levels of survivin were assessed by RT-PCR and western blot, respectively. GAPDH and β-actin were used as controls. (C) Survivin promoter-dependent activity by using the reporter vectors pLuc-1710 (survivin promoter containing Tcf/Lef binding sites) and pLuc-420-3M (mutated Tcf/Lef binding sites). Results were calculated using the ratio 1710/420 for all conditions. (*) Statistically significant differences from 3 independent experiments (bars indicate standard error).

overexpressing β-catenin S646D displayed the narrowest distribution of volumes, having 60% of granules between 0.05 and 0.15 μm^3 and lacking granules larger than 0.4 μm^3. To show the most important differences in volume distribution, volumes were divided into three intervals (in μm^3) and were depicted together a 3D-model of each condition (Fig. 5B,C).

2.4. β-Catenin S646D is more retained in the nucleus

Since β-catenin is known can shuttle between the nucleus and cytoplasm without the need of other soluble factors, we aimed to analyze the movement of the two β-catenin variants by doing FRAP experiments in live cells, and particularly its relationship with the granule number, volume and area values observed. Initially, analysis of nuclear import rates of β-catenin variants was chosen, but the high level of fluorescence in the nucleus made very difficult the bleaching of this compartment. Thus, nuclear export rate was evaluated by bleaching the cytoplasm, as observed in Fig. 6A. After measuring the recovery of the fluorescence for 300 s, recovery curves normalized against the pre-bleach and the whole cell fluorescence intensities were plotted. Fluorescence recovery was moderated for all conditions, reaching around 40% of pre-bleach fluorescence (Fig. 6B). Finally, nuclear export rates from recovery curves were calculated by fitting the data to an exponential equation, which it allowed to calculate the Tau (τ) value that represents the time where fluorescence intensity reaches 50% recovery (Fig. 6C). Alternatively, nuclear export rate was also determined by calculating the slopes after fitting the first 30 s of the curves to a linear equation (data not shown). By using both methods, despite β-catenin S646D displayed a higher tendency that WT, nuclear export rates did not show significant differences.

3. Discussion

In this work, we have evaluated whether the chemical nature of the residue 646 of human β-catenin had a role on its subcellular localization, transport between the cytoplasm and nucleus, and transactivating activity. One particular finding in this work was the formation of nuclear granules of β-catenin-GFP. These β-catenin aggregates differ morphologically from previously observed β-catenin nuclear aggregates in Cos-7 cells, which presented a rod-shaped structure with sharp tips (Giannini et al., 2000), however were similar to the speckle-like structures observed by Simcha and colleagues, although they also reported rod-like aggregates (Simcha et al., 1998). Kim and colleagues found in NIH-3T3 cells rounded aggregates of β-catenin which high magnification revealed as ring-shaped structures (Kim and Hay, 2001).

We did observe ring-shaped aggregates, but most of them presented a rounded solid morphology. In all previous studies β-catenin was exogenously expressed and although two of the three reports that describe β-catenin nuclear aggregates used our same construct, it seems that they formed independently of the GFP moiety, since one report presented aggregates with a similar rounded morphology with a VSV-tagged β-catenin (Simcha et al., 1998). Recently, endogenous β-catenin was shown to be localized at Promyelocytic Leukemia Nuclear Bodies

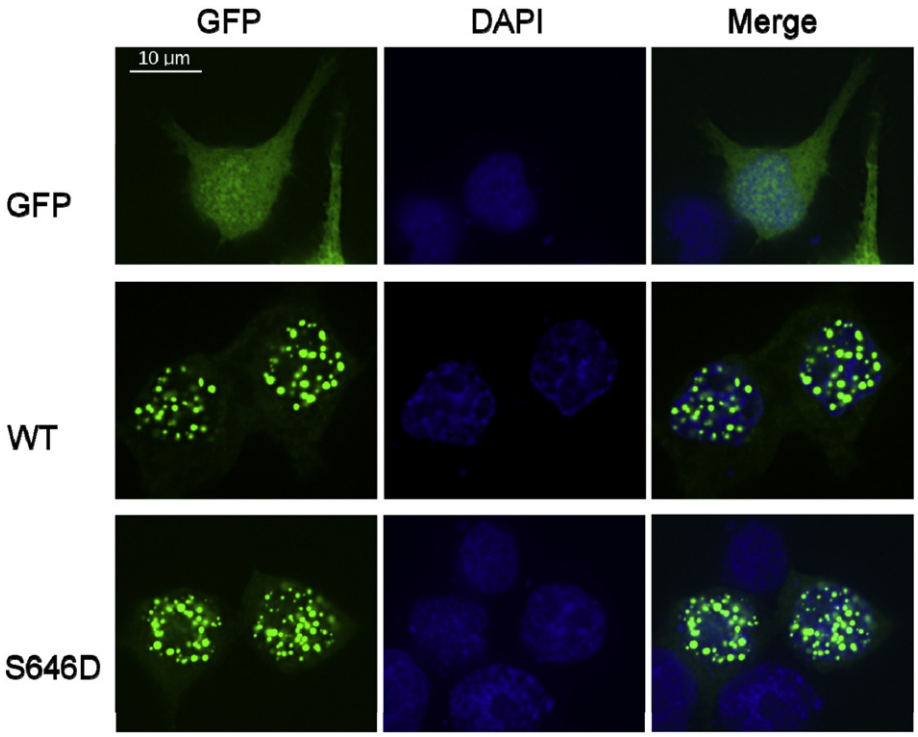

Fig. 3. Nuclear clustering of β-catenin S646D. HEK-293T cells were transfected with plasmids as in Fig. 2A and used pEGFP-C1 plasmid as negative control. Cells were grown on coverslips for 24 h, fixed and then GFP-derived fluorescence was analyzed by confocal microscopy using a 60× lens.

(PML-NBs) in osteoblast tumor cells, forming a punctuate nuclear pattern (Zhang et al., 2014). Many foreign and overexpressed proteins have been found to localize to PML-NBs and subsequently are degraded (Dellaire et al., 2004; Tsukamoto et al., 2000). Whether overexpressed β-catenin is localizing into these nuclear bodies and being degraded is an interesting and unexplored possibility.

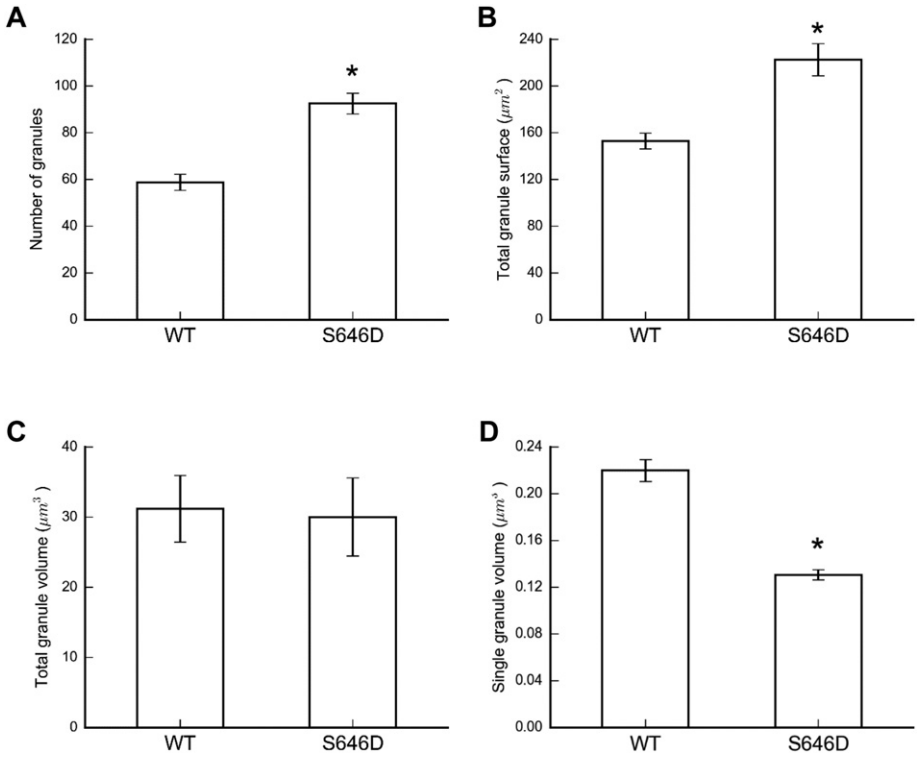

Fig. 4. Spatial parameters of β-catenin S646D-derived granules. HEK-293T cells were transfected as in Fig. 3. Z-stacks of step-size. Three-dimensional models of nuclei were constructed on the basis of 15 images taken at $\Delta z = 300$ nm. Number of granules per nucleus (A), nuclear area covered by granules (B), nuclear volume of the granules (C) and single granule volume (D) were calculated as mentioned in Material and methods. Mean values and standard errors are calculated from at least 30 cells per experiment (*$p < 0.05$).

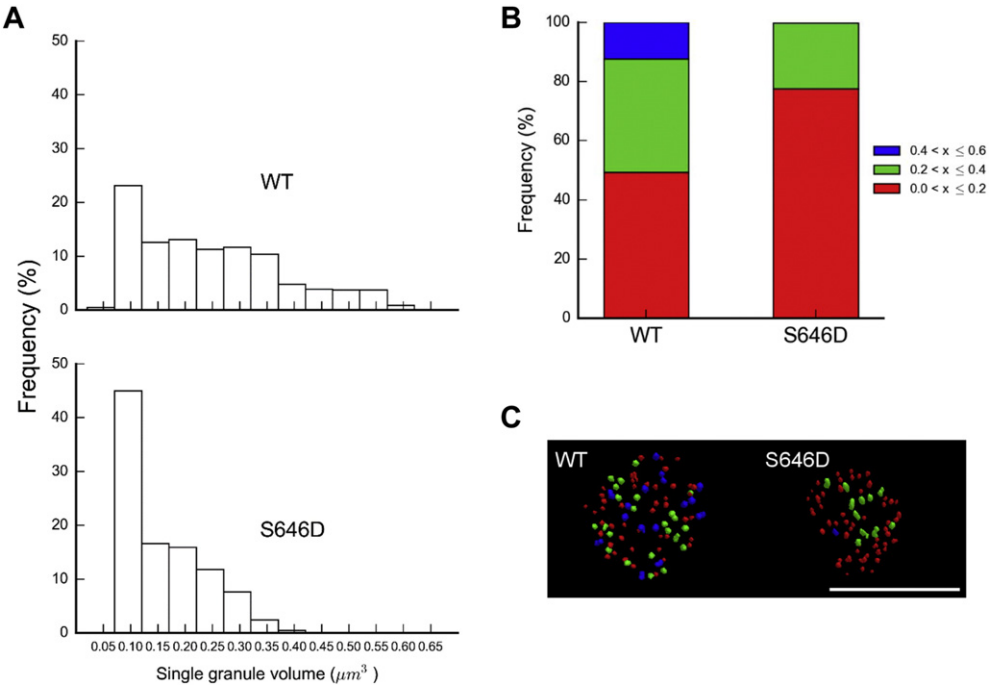

Fig. 5. Distribution of nuclear granules of β-catenin S646D. HEK-293T cells treated as in Fig. 4 were analyzed according to their single granule volume distribution. (A) Frequency (%) of single granule volume distribution. (B) Single granule volume distribution represented with three colored volume ranges in μm^3. (C) A representative model of each nucleus expressing β-catenin WT and S646D, where granules were colored according their single granule volume color code shown in B. Bar = 10 μm.

Protein misfolding is among the reasons that can contribute to protein aggregation. Most protein aggregation occurs between unfolded or partially folded proteins (Ellis and Minton, 2006). Although our experiments did not rule out the possibility to have partially folded proteins, the TCF/LEF reporter activity of the β-catenin variants was considerably higher than the negative control. Since the TCF/LEF binding

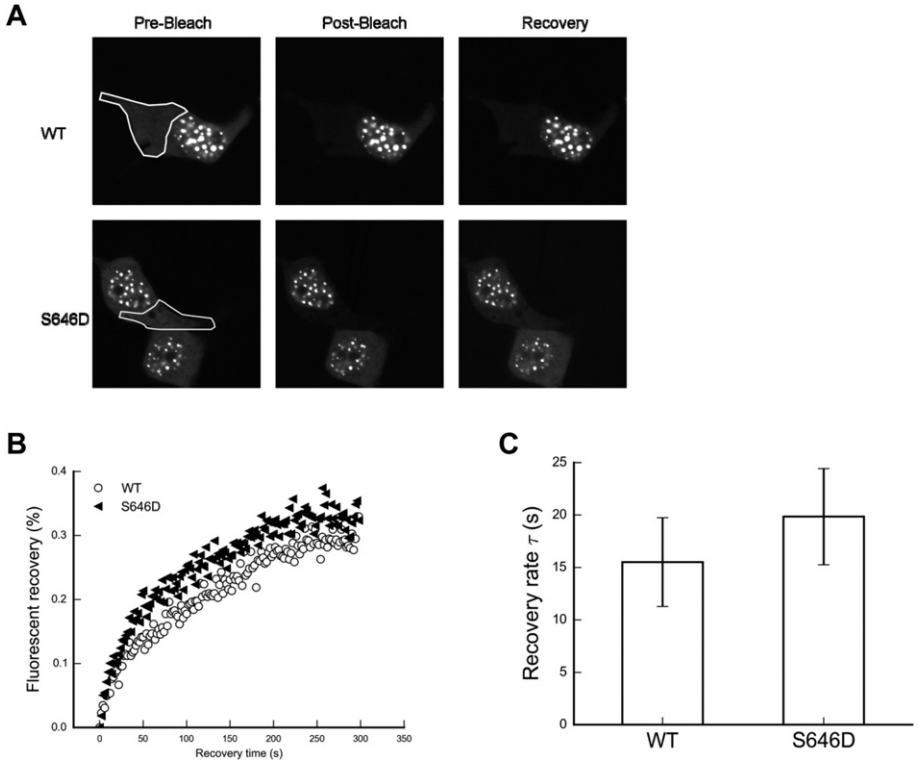

Fig. 6. Nuclear export rate of β-catenin S646D. HEK-293T cells were transfected as in Fig. 3, then were grown on coverslips for 20 h and further analyzed by time-lapse microscopy for FRAP. (A) Live cell images of a representative FRAP experiment. In the pre-bleach condition is depicted the bleached region. In all experiments, about 90% of the cytoplasm was bleached. (B) Cytoplasmic fluorescence recovery curves for β-catenin WT and S646D. At least 5 different cells were analyzed for the calculation of each curve and the fluorescence recovery was measured for 300 s. (C) Nuclear export of β-catenin WT and S646D by comparing the rates (tau, τ) calculated from the curves presented in (B) and fitted to the equation $y = A(1 - e^{-\tau t1/2})$, where A is the plateau of the curve and $t_{1/2}$ is the time where half of the recovery curve has been reached.

domain of β-catenin comprises a large region of its structure, R3–R10 (Graham et al., 2000), as well as efficient nuclear import activity of β-catenin depends on R10–R12 (Koike et al., 2004), we believe that both overexpressed β-catenins WT and S646D can be properly folded.

In addition, excess of β-catenin in a limited volume like the nucleus cannot be ruled out to contribute to the formation of the protein aggregates. The high fluorescence intensities and dense distribution of the granules observed throughout the nucleus is indicative of a high concentration of this protein. This could have thus contributed to the highly crowded environment found into this compartment, thereby facilitating the formation of these protein aggregates given that crowding is long-time known to enhance protein association (Zimmerman and Minton, 1993).

Our results show that β-catenin accumulated exclusively into the nucleus forming a granular pattern that did not change over time, which suggested its retention into this compartment. This retention effect has been previously described for LEF-1, TCF4 and BCL9, which also induces β-catenin nuclear retention (Jamieson et al., 2011; Krieghoff et al., 2006). According the reported crystal structure, aspartic acid in position 646 should not interfere with binding between β-catenin and TCF/LEF factors (Graham et al., 2000). Furthermore, once in the nucleus, β-catenin binds to various proteins involved in gene regulation, including histone remodeling factors BRG1 and ISW1, histone acetyltranferases CBP and p300, as well as parafibromin and the aforementioned PML-NBs, all proteins that may anchor β-catenin to active transcriptional regions into the chromatin (Mosimann et al., 2009). Altogether, these proteins may enhance the retention of β-catenin into the nucleus, however, our experiments did no assess whether these granules were indeed bound to chromatin.

Both β-catenin wild-type and S646D formed the same total volume of aggregates in the nucleus but the number of granules and thereby the covered area were different. Covered area arises as an interesting feature because represents the surface accessible to other proteins, opening the possibility to find differences in the nuclear export rates of β-catenin. Despite export rates were not significantly different between both β-catenin forms, which indicates that chemical nature of residue 646 appears not affect this feature, that an excess of β-catenin protein into the nucleus could overpass control mechanisms thus avoiding potential differences in export rates, is an interesting possibility that cannot be ruled out as well.

4. Materials and methods

4.1. General

Cell medium and antibiotics were purchased from Invitrogen (Paisley, UK). Fetal bovine serum (FBS) was from HyClone (Logan, UT). RIPA buffer and BCA protein kit were from Thermo Scientific (Rockford, IL). Plasmid Midiprep kit was from Qiagen (Valencia, CA). NitroPure membrane was from Macherey-Nagel (Düren, Germany). Lipofectamine 2000 was from Life Technologies (Rockford, IL). Buffers and all other reagents used, but not specified, were from Sigma-Aldrich or the highest grade available.

4.2. Plasmids

β-Catenin S646D was designed using primers forward 5′-actccacgacaggaatgaag-3′ and reverse 5′-cttcattcctgtcgtggagt-3′, following the manufacturer's instructions (The GeneArt® Site-Directed Mutagenesis System, Invitrogen). β-Catenin wild-type and S646D were cloned into SacII/XbaI sites of pEGFP-C1 (Clontech, CA, USA). Reporter plasmids pLuc-1710 (containing the survivin promoter with Tcf/Lef binding sites) and pLuc-420-3M (mutated Tcf/Lef binding sites) were previously described (Ponce et al., 2011).

4.3. Cell culture and transfection

HEK-293T cells were cultured at 37 °C and 5% CO_2 in DMEM supplemented with 10% FBS and antibiotics (10,000 units/ml penicillin and 10 μg/ml streptomycin). Transfection was carried out using the Superfect Transfection Reagent (Qiagen), following instructions of manufacturer. Cells were grown at 70% confluence at the moment of transfection and 20 h after were analyzed by RT-PCR, western blot and confocal microscopy.

4.4. Confocal microscopy and 3D-modeling

GFP-β-cat-WT or GFP-β-cat-S646D expressing cells were grown on coverslips for 20 h and visualized in a spinning disk confocal microscope (IX81, Olympus) equipped with a 12-bit CCD camera (XM10, Olympus). Z-stacks of single cells were obtained taking 10 images at a step size of 300 nm. The 3D-models of single nuclei were build using image-processing routines developed in SCIAN laboratory (www.scian.cl) based on interactive data language (IDL, ITT, Boulder, Colorado) as described in Liddle et al. (2014). These routines included consecutive ROI segmentation stages, obtaining 3D-models of single nuclei and afterward granules, and finally quantification of their number, area and volume (Castañeda et al., 2014). Models of 30 cells per β-catenin variant were analyzed.

4.5. Fluorescence recovery after photo bleaching

GFP-β-cat-WT or GFP-β-cat-S646D expressing cells were grown on coverslips for 20 h and then analyzed in a FV-1000 Fluoview confocal microscope (Olympus). Using a 60× objective (NA 1.35, oil immersion) and a 473 nm excitation laser, one pre-bleach image was acquired and then laser was set at 100% power until 90% of the cytoplasm was bleached (10–15 s depending on fluorescence intensity). After bleaching, consecutive frames were taken at 1.2 s intervals for approximately 300 s. Background values were subtracted from every image and the averaged fluorescence intensity in the bleached area to the whole cell was plotted. For every analyzed cell, the fluorescence ratio of the pre-bleach image was set to 100% and the first frame after bleaching was set as time point 0. At least 5 different cells were analyzed for the calculation of each curve. Nuclear export rate from the recovery curves was calculated by fitting the curves to the exponential equation $y = A(1 - e^{-\tau t})$, where A represents the plateau of the curve and $\tau_{1/2}$ the half of recovery rate, which is the time point where half of the recovery curve has been reached.

4.6. Analysis of mRNA levels by RT-PCR

RNA was isolated from cells with Trizol reagent following the manufacturer's instructions. Cellular mRNA was used to detect survivin (5′-ccgacgttgccccctgc-3′ and 5′-ggccatccacagtcttct-3′) and GAPDH (5′-ccttcattgacctcaacta-3′ and 5′-ggccatccacagtcttct-3′) by RT-PCR. Reaction products were analyzed after 30 amplification cycles in 2% agarose gels containing ethidium bromide.

4.7. Analysis of protein levels by western blot

Cell lysates were prepared with RIPA Lysis and Extraction Buffer (Thermo Scientific) and 30 μg total proteins were loaded per lane in 12% SDS-PAGE minigels (Bio-Rad), and then transferred to a nitrocellulose film. Blots were blocked with 5% milk in 0.1% Tween–phosphate-buffered saline (PBS) and then probed with anti-actin (dilution, 1:5000) and anti-survivin (1:3000) antibodies. Bound antibodies were detected with horseradish peroxidase-conjugated secondary antibodies and the enhanced chemiluminescence system (EZ-ECL).

4.8. Luciferase reporter assay

Cells were transfected with 15 μg total DNA of the combinations pLuc-1710/pLuc-420-3M plus the plasmids encoding GFP-β-cat-WT or GFP-β-cat-S646D forms as indicated. Cells were lysed 24 h post-transfection in a buffer containing 100 mM KH_2PO_4 (pH 7.9), 1 mM DTT and 0.5% Triton X-100. Aliquots of supernatants obtained after extraction and centrifugation were used to measure luciferase activity with the substrate luciferin following instructions provided by the manufacturer (Promega). The values reported for luciferase activity for each condition were used for calculating the pLuc-1710/420-3M activity ratios. Values shown were averaged from at least three independent experiments. Ectopic protein expression was usually checked by western blotting with specific antibodies.

4.9. Statistical analysis

Data were compared using the Dunnett's or Student's methods after ANOVA. A value for $P < 0.05$ was considered significant.

Competing financial interests

The authors declare no conflicts of interest.

Acknowledgments

Supported by grants from the Fondo Nacional de Desarrollo Cientifico y Tecnologico-FONDECYT 1120132 and the International Centre for Genetic Engineering and Biotechnology-ICGEB CRP/CHI10-01 (to JCT); FONDECYT 1151029, FONDEF D11I1096, DAAD and ICM P09-015-F (to SH); The Centro de Estudios Cientificos is funded by the Chilean Government through the Centers of Excellence Basal Financing Program of CONICYT (to LFB).

We thank Omar Ramirez (SCIAN-Lab) for his important technical advice.

Contribution to the work: JLM, IN, ES, HH and RC performed the experiments; JLM, SH, LFB and MG analyzed the data; JLM and JCT wrote the manuscript; JCT designed the study.

References

Ahmed, K., Gerber, D.A., Cochet, C., 2002. Joining the cell survival squad: an emerging role for protein kinase CK2. Trends Cell Biol. 12, 226–230.

Apopa, P.L., He, X., Ma, Q., 2008. Phosphorylation of Nrf2 in the transcription activation domain by casein kinase 2 (CK2) is critical for the nuclear translocation and transcription activation function of Nrf2 in IMR-32 neuroblastoma cells. J. Biochem. Mol. Toxicol. 22, 63–76.

Bienz, M., Clevers, H., 2000. Linking colorectal cancer to Wnt signaling. Cell 103, 311–320.

Castañeda, V., Cerda, M., Santibañez, F., Jara, J., Pulgar, E., Palma, K., Lemus, C.G., Concha, M., Härtel, S., 2014. Computational methods for analysis of dynamic events in cell migration. Curr. Mol. Med. 14 (2), 291–307.

Cook, A., Bono, F., Jinek, M., Conti, E., 2007. Structural biology of nucleocytoplasmic transport. Annu. Rev. Biochem. 76, 647–671.

Cong, F., Varmus, H., 2004. Nuclear-cytoplasmic shuttling of Axin regulates subcellular localization of β-catenin. Proc. Natl. Acad. Sci. U. S. A. 101, 2882–2887.

De Abreu da Silva, I.C., Carneiro, V.C., Maciel, R.D.M., da Costa, R.F.M., Furtado, D.R., de Oliveira, F.M.B., da Silva-Neto, M.A.C., Rumjanek, F.D., Fantappié, M.R., 2011. CK2 phosphorylation of *Schistosoma mansoni* HMGB1 protein regulates its cellular traffic and secretion but not its DNA transactions. PLoS ONE 6, e23572.

Dellaire, G., Bazett-Jones, D.P., Bazett-Jones, D.P., 2004. PML nuclear bodies: dynamic sensors of DNA damage and cellular stress. BioEssays 26, 963–977.

Eleftheriou, A., Yoshida, M., Henderson, B.R., 2001. Nuclear export of human β-catenin can occur independent of CRM1 and the adenomatous polyposis coli tumor suppressor. J. Biol. Chem. 276, 25883–25888.

Ellis, R.J., Minton, A.P., 2006. Protein aggregation in crowded environments. Biol. Chem. 387, 48597.

Gao, Y., Wang, H., 2006. Casein kinase 2 Is activated and essential for Wnt/β-catenin signaling. J. Biol. Chem. 281, 18394–18400.

Giannini, A.L., Vivanco, M.M., Kypta, R.M., 2000. Analysis of beta-catenin aggregation and localization using GFP fusion proteins: nuclear import of alpha-catenin by the beta-catenin/Tcf complex. Exp. Cell Res. 255, 207–220.

Graham, T.A., Weaver, C., Mao, F., Kimelman, D., Xu, W., 2000. Crystal structure of a β-catenin/Tcf complex. Cell 103, 885–896.

Henderson, B.R., 2000. Nuclear-cytoplasmic shuttling of APC regulates β-catenin subcellular localization and turnover. Nat. Cell Biol. 2, 653–660.

Henderson, B.R., Fagotto, F., 2002. The ins and outs of APC and β-catenin nuclear transport. EMBO Rep. 3, 834–839.

Jamieson, C., Sharma, M., Henderson, B.R., 2011. Regulation of β-catenin nuclear dynamics by GSK-3b involves a LEF-1 positive feedback loop. Traffic 12, 1–17.

Jamieson, C.H.M., Ailles, L.E., Dylla, S.J., Muijtjens, M., Jones, C., Zehnder, J.L., Gotlib, J., Li, K., Manz, M.G., Keating, A., Sawyers, C.L., Weissman, I.L., 2004. Granulocyte–macrophage progenitors as candidate leukemic stem cells in blast-crisis CML. N. Engl. J. Med. 351, 657–667.

Kim, K., Hay, E.D., 2001. New evidence that nuclear import of endogenous beta-catenin is LEF-1 dependent, while LEF-1 independent import of exogenous beta-catenin leads to nuclear abnormalities. Cell Biol. Int. 25, 1149–1161.

Koike, M., Kose, S., Furuta, M., Taniguchi, N., Yokoya, F., Yoneda, Y., Imamoto, N., 2004. β-Catenin shows an overlapping sequence requirement but distinct molecular interactions for its bidirectional passage through nuclear pores. J. Biol. Chem. 279, 34038–34047.

Krieghoff, E., Behrens, J., Mayr, B., 2006. Nucleo-cytoplasmic distribution of β-catenin–catenin is regulated by retention. J. Cell Sci. 119, 1453–1463.

Lee, S.J., Imamoto, N., Sakai, H., Nakagawa, A., Kose, S., Koike, M., Yamamoto, M., Kumasaka, T., Yoneda, Y., Tsukihara, T., 2000. The adoption of a twisted structure of importin-beta is essential for the protein–protein interaction required for nuclear transport. J. Mol. Biol. 302, 251–264.

Liddle, P., Lafon-Hughes, L., Di Tomaso, M.V., Reyes-Ábalos, A.L., Jara, J., Cerda, M., Härtel, S., Folle, G., 2014. Bleomycin-induced yH2AX foci map preferentially to replicating domains in CHO9 interphase nuclei chromosome research. CHRS-s-13-00133 http://dx.doi.org/10.1007/s10577-014-9433-9.

Litchfield, D.W., 2003. Protein kinase CK2: structure, regulation and role in cellular decisions of life and death. Biochem. J. 369, 1–15.

Logan, C.Y., Nusse, R., 2004. The Wnt signaling pathway in development and disease. Annu. Rev. Cell Dev. Biol. 20, 781–810.

Macdonald, B.T., Tamai, K., He, X., 2009. Wnt/β-catenin signaling: components, mechanisms, and diseases. Dev. Cell 17, 9–26.

Meggio, F., Pinna, L.A., 2003. One-thousand-and-one substrates of protein kinase CK2? FASEB J. 17, 349–368.

Mosimann, C., Hausmann, G., Basler, K., 2009. β-catenin hits chromatin: regulation of Wnt target gene activation. Nat. Rev. Mol. Cell Biol. 10, 276–286.

Neufeld, K.L., Zhang, F., Cullen, B.R., White, R.L., 2000. APC-mediated downregulation of β-catenin activity involves nuclear sequestration and nuclear export. EMBO Rep. 1, 519–523.

Panasyuk, G., Nemazanyy, I., Zhyvoloup, A., Bretner, M., Litchfield, D.W., Filonenko, V., Gout, I.T., 2006. Nuclear export of S6K1 II is regulated by protein kinase CK2 phosphorylation at Ser-17. J. Biol. Chem. 281, 31188–31201.

Plotnikov, A., Chuderland, D., 2011. Nuclear extracellular signal-regulated kinase 1 and 2 translocation is mediated by casein kinase 2 and accelerated by autophosphorylation. Mol. Cell. Biol. 31, 3515–3530.

Ponce, D.P., Maturana, J.L., Cabello, P., Yefi, R., Niechi, I., Silva, E., Armisen, R., Galindo, M., Antonelli, M., Tapia, J.C., 2011. Phosphorylation of AKT/PKB by CK2 is necessary for the AKT-dependent up-regulation of beta-catenin transcriptional activity. J. Cell. Physiol. 226, 1953–1959.

Porter, C.M., Havens, M., a, Clipstone, N. a,, 2000. Identification of amino acid residues and protein kinases involved in the regulation of NFATc subcellular localization. J. Biol. Chem. 275, 3543–3551.

Quélo, I., Gauthier, C., St-Arnaud, R., 2005. Casein kinase II phosphorylation regulates alphaNAC subcellular localization and transcriptional coactivating activity. Gene Expr. 12, 151–163.

Rosin-Arbesfeld, R., Cliffe, A., Brabletz, T., Bienz, M., 2003. Nuclear export of the APC tumour suppressor controls beta-catenin function in transcription. EMBO J. 22, 1101–1113.

Seldin, D.C., Landesman-Bollag, E., Farago, M., Currier, N., Lou, D., Dominguez, I., 2005. CK2 as a positive regulator of Wnt signalling and tumourigenesis. Mol. Cell. Biochem. 274, 63–67.

Simcha, I., Shtutman, M., Salomon, D., Zhurinsky, J., Sadot, E., Geiger, B., Ben-Ze'ev, A., 1998. Differential nuclear translocation and transactivation potential of beta-catenin and plakoglobin. J. Cell Biol. 141, 1433–1448.

Song, D.H., Dominguez, I., Mizuno, J., Kaut, M., Mohr, S.C., Seldin, D.C., 2003. CK2 phosphorylation of the armadillo repeat region of β-catenin potentiates Wnt signaling. J. Biol. Chem. 278, 24018–24025.

Tapia, J., Torres, V., Rodriguez, D., Leyton, L., Quest, A., 2006. Casein kinase 2 (CK2) increases survivin expression via enhanced β-catenin–T cell factor/lymphoid enhancer binding factor-dependent transcription. Proc. Natl. Acad. Sci. U. S. A. 103, 15079–15084.

Thyssen, G., Li, T.-H., Lehmann, L., Zhuo, M., Sharma, M., Sun, Z., 2006. LZTS2 is a novel beta-catenin-interacting protein and regulates the nuclear export of beta-catenin. Mol. Cell. Biol. 26, 8857–8867.

Townsley, F.M., Cliffe, A., Bienz, M., 2004. Pygopus and legless target armadillo/β-catenin to the nucleus to enable its transcriptional co-activator function. Nat. Cell Biol. 6, 626–633.

Tsukamoto, T., Hashiguchi, N., Janicki, S.M., Tumbar, T., Belmont, A.S., Spector, D.L., 2000. Visualization of gene activity in living cells. Nat. Cell Biol. 2, 871–878.

Wang, A., Wang, J., Ren, H., Yang, F., Sun, L., Diao, K., Zhao, Z., Song, M., Cui, Z., Wang, E., Wei, M., Mi, X., 2014. TRAF4 participates in Wnt/β-catenin signaling in breast cancer by upregulating β-catenin and mediating its translocation to the nucleus. Mol. Cell. Biochem. 395, 211–219.

Wiechens, N., Fagotto, F., 2001. CRM1-and Ran-independent nuclear export of β-catenin. Curr. Biol. 11, 18–28.

Xing, Y., Takemaru, K., Liu, J., Berndt, J., Zheng, J., Moon, R.T., Xu, W., 2008. Crystal structure of a full-length β-catenin. Structure 16, 478–487.
Yefi, R., Ponce, D.P., Niechi, I., Silva, E., Cabellom, P., Rodriguez, D.A., Marcelain, K., Armisen, R., Quest, A.F., Tapia, J.C., 2011. Protein kinase CK2 promotes cancer cell viability via up-regulation of cyclooxygenase-2 expression and enhanced prostaglandin E2 production. J. Cell. Biochem. 112, 3167–3175.
Zhang, F., White, R., Neufeld, K., 2001a. Cell density and phosphorylation control the subcellular localization of adenomatous polyposis coli protein. Mol. Cell. Biol. 21, 8143–8156.
Zhang, M., Mahoney, E., Zuo, T., Manchanda, P.K., Davuluri, R.V., Kirschner, L.S., 2014. Protein kinase A activation enhances β-catenin transcriptional activity through nuclear localization to PML bodies. PLoS ONE 9, e109523.
Zhang, N., Wei, P., Gong, A., Chiu, W., Lee, H., 2011. FoxM1 promotes β-catenin nuclear localization and controls Wnt target-gene expression and glioma tumorigenesis. Cancer Cell 20, 427–442.
Zhang, T., Otevrel, T., Gao, Z., Gao, Z., Ehrlich, S.M., Fields, J.Z., Boman, B.M., 2001b. Evidence that APC regulates survivin expression: a possible mechanism contributing to the stem cell origin of colon cancer. Cancer Res. 61, 8664–8667.
Zimmerman, S., Minton, A., 1993. Macromolecular crowding: biochemical, biophysical, and physiological consequences. Annu. Rev. Biophys. 22, 27–65.